

*Third International Symposium on the Effects of Surface Geology on Seismic Motion
Grenoble, France, 30 August - 1 September 2006
Paper Number: xxx*

AN EFFICIENT ADER-DG METHOD FOR 3-DIMENSIONAL SEISMIC WAVE PROPAGATION IN MEDIA WITH COMPLEX GEOMETRY

Martin KÄSER¹, Michael DUMBSE^{1,2}, Josep DE LA PUENTE³

1 Department of Civil and Environmental Engineering, University of Trento, Trento, Italy

2 Institut für Aerodynamik und Gasdynamik, Universität Stuttgart, Stuttgart, Germany

3 Department of Earth and Environmental Sciences, Universität München, München, Germany

ABSTRACT - We present a new numerical method to simulate seismic wave propagation in geometrically complex three-dimensional viscoelastic media with high order accuracy in space and time. The scheme solves the seismic wave equations formulated as a linear hyperbolic system on three dimensional unstructured tetrahedral meshes by combining the Discontinuous Galerkin Finite Element method with a new time integration approach using arbitrary high order derivatives of the solution for flux calculation. In contrast to classical Finite Element methods, the numerical solution is approximated by piecewise polynomials which allow for discontinuities at element interfaces and shows spectral convergence even on unstructured tetrahedral meshes. Due to the local character of the numerical scheme and the particular time integration approach, the approximation order can be chosen adaptively and a local time stepping technique can be applied. Together with an appropriate mesh partitioning technique, we improve the efficiency of the proposed method considerably without losing the desired high order accuracy or the flexibility provided by an unstructured tetrahedral mesh. To confirm its performance we finally apply the new scheme to the 3-D benchmark simulation of the Grenoble valley.

1. Introduction

The solution of the seismic wave equations with very high accuracy in space and time is still a challenging task, especially for realistic models including complex 3-D geometries like surface topography or non-planar internal boundaries and material interfaces. Furthermore, attenuation and dispersion, which strongly affect the seismic wave field, have to be considered to correctly model the wave amplitudes and phases of a fully 3-D seismic wave field. Realistic attenuation properties are obtained by incorporating viscoelastic media that combine the behaviour of elastic solids and viscous fluids.

A new approach, combining the Discontinuous Galerkin (DG) method of (Reed and Hill, 1973) with a time integration method using Arbitrary high order DERivatives (ADER) as introduced in (Toro et al., 2001; Titarev and Toro, 2002), was proposed in (Dumbser, 2005) for linear hyperbolic systems. This highly accurate numerical method was then introduced for the simulation of elastic wave propagation on unstructured meshes for two and three space dimensions (Käser and Dumbser, 2006; Dumbser and Käser, 2006). The presented ADER-DG schemes approximate the unknown solution inside each tetrahedral element by a polynomial, whose coefficients - the degrees of freedom - are advanced in time. Hereby, the polynomial representation of the solution can be discontinuous across the element interfaces, which allows to incorporate the well-established ideas of

numerical flux functions from the Finite Volume (FV) framework. To define a suitable flux over the element surfaces a so-called Generalized Riemann Problem (GRP) (Toro et al., 2001) is solved at the element interfaces, which provides simultaneously a time-integration method. The main idea is a Taylor expansion in time in which all time derivatives are replaced by space derivatives using the so-called Cauchy-Kovalevski procedure which makes extensive use of the governing PDE. The numerical solution can thus be advanced for one time step without intermediate stages in contrast to classical multi-stage Runge-Kutta time stepping schemes. Furthermore, the projection of the tetrahedral elements in physical space onto a canonical reference tetrahedron allows for an efficient implementation, as many computations of three-dimensional integrals can be carried out analytically beforehand.

Later, this scheme was extended to viscoelastic rheologies in (Käser et al., 2006), where additional anelastic functions are incorporated resulting from different attenuation mechanisms of a generalized Maxwell body (Emmerich and Korn, 1987; Carcione et al., 1988). This way, realistic seismic wave field attenuation and dispersion is modeled correctly. Hereby, it is important that the earth's internal friction, i.e. the measure of attenuation, is nearly constant over a wide seismic frequency range, which is due to the composition of the earth's polycrystalline material consisting of different minerals. The superposition of these microscopic physical attenuation processes generally leads to a flat attenuation band.

In this paper, we present important extensions of this ADER-DG approach as far as its applicability and efficiency to realistic, large scale applications is concerned. The degree P of the approximation polynomials determines the order of accuracy of the numerical scheme. As most problems include zones of high and low interest a globally high degree P is not required and unnecessarily increases computational run time. Therefore, a P -adaptive ADER-DG approach is introduced, where different polynomial degrees P can be chosen for individual tetrahedral elements. The flux computation across an element interface requires a matrix-matrix multiplication of the flux-matrix and the matrix containing the degrees of freedom. Due to an hierarchical order of the polynomial basis functions the flux-matrices of a lower order element represent a subset of these matrices of a higher order element. This way, a P -adaptive flux calculation only uses the necessary part of these matrices and therefore enhances computational efficiency. A further important extension is the use of a local time step in the individual elements, such that each element uses its maximum time step allowed by the stability criterion. This way, small elements have to be updated with a small time step frequently, whereas large elements have to be updated less often. Therefore, small tetrahedrons that might appear due to complex geometrical features or due to high spatial resolution requirements to not globally restrict the time step. Furthermore, a new mesh partition technique has been developed in order to achieve better load balancing for MPI parallelisation of the P -adaptive ADER-DG schemes with local time stepping. Thus, the mesh is split into different zones which might be determined by geometrical features. Then each of these zones is partitioned into a number of subdomains that is determined by the number of available processors.

Finally, we apply the proposed ADER-DG scheme with its full functionality to the numerical benchmark of 3-D ground motion simulation in the valley of Grenoble and present your results in form of seismograms and a 2-D map of surface peak ground particle velocity.

2. The Numerical Scheme

The proposed numerical method combines a Discontinuous Galerkin (DG) Finite Element scheme with a time integration technique using Arbitrarily high order DERivatives (ADER) in order to solve the governing PDE with arbitrarily high approximation order in time and space. The system of the three-dimensional seismic wave equations formulated in velocity-stress leads to a hyperbolic system of the form

$$\frac{\partial Q_p}{\partial t} + A_{pq} \frac{\partial Q_q}{\partial \xi} + B_{pq} \frac{\partial Q_q}{\partial \eta} + C_{pq} \frac{\partial Q_q}{\partial \zeta} = 0, \quad (1)$$

where the vector Q of unknowns contains the six stress and the three velocity components. The Jacobian matrices A , B and C include the material values as explained in detail in (Käser and Dumbser, 2006; Dumbser and Käser, 2006). As described in detail in (Dumbser and Käser, 2006) in the Discontinuous Galerkin approach the solution is approximated inside each tetrahedron by a linear combination of space-dependent polynomial basis functions and time-dependent degrees of freedom as expressed through

$$(Q_h)_p(\xi, \eta, \zeta, t) = \hat{Q}_{pl}(t) \Phi_l(\xi, \eta, \zeta), \quad (2)$$

where the basis functions Φ_l form a orthogonal basis and are defined on the canonical reference tetrahedron. As deriving the numerical scheme in detail would go beyond the scope of this paper, we refer to previous work in (Käser and Dumbser, 2006; Dumbser and Käser, 2006) for a detailed mathematical formulation of the Discontinuous Galerkin method. However, we mention that the time accuracy of the scheme is automatically equal to the space accuracy determined by the degree of approximation polynomials used in equation (2). This is due to the ADER time integration approach, where the fundamental idea is to expand the solution via a Taylor series of order $(N-1)$ in time

$$Q_p(\xi, \eta, \zeta, t) = \sum_{k=0}^N \frac{t^k}{k!} \frac{\partial^k}{\partial t^k} Q_p(\xi, \eta, \zeta, 0), \quad (3)$$

where we then replace all time derivatives in equation (3) by space derivatives using the governing PDE in equation (1). It can be shown that the k -th time derivative can be expressed as

$$\frac{\partial^k}{\partial t^k} Q_p = (-1)^k \left(A_{pq} \frac{\partial}{\partial \xi} + B_{pq} \frac{\partial}{\partial \eta} + C_{pq} \frac{\partial}{\partial \zeta} \right)^k Q_q, \quad (4)$$

and therefore using equation (4) in (3) the Taylor series only depends on space derivatives of the basis functions Φ_l of equation (2) and the degrees of freedom from the actual, i.e. local time level 0, as finally given by

$$Q_p(\xi, \eta, \zeta, t) = \sum_{k=0}^N \frac{t^k}{k!} (-1)^k \left(A_{pq} \frac{\partial}{\partial \xi} + B_{pq} \frac{\partial}{\partial \eta} + C_{pq} \frac{\partial}{\partial \zeta} \right)^k Q_q(\xi, \eta, \zeta, 0). \quad (5)$$

The expression in equation (5) can be integrated in time analytically as shown in detail in (Dumbser and Käser, 2006) and therefore leads to a new approach termed ADER-DG method that provided arbitrarily high order in space and time depending on the degree of the basis polynomials Φ_l in equation (2) and the corresponding order $(N-1)$ of the time Taylor series in , chosen in equation (3). However, the accuracy of the schemes is

computationally costly as a many matrix-matrix multiplications have to be carried to evolve the degrees of freedom in time. Therefore, different approaches to enhance computational efficiency, in particular for parallel computing, are addressed in the following.

3. Increasing Computational Efficiency

For large scale applications computational efficiency is essential in order to obtain a desired accuracy of the results in a reasonable time. There are many different possibilities to reduce computational cost, however, we remark that the key issue of our approach is to preserve the high order accuracy and spectral convergence of the proposed ADER-DG schemes.

3.1. *P*-Adaptivity

In most applications, the computational domain is larger than a particular zone of interest, often also to avoid effects from the boundaries. Therefore, a large number of elements is needed to discretize the entire geometry of the model. However, as in most cases the high order accuracy is only required in a restricted area of the computational domain, it is desirable to choose the accuracy adaptively in space. This means, that it must be possible to vary the degree P of the approximation polynomials Φ_i in equation (2) from one element to the other. Furthermore, due to a hierarchical order of the basis functions the degrees of freedom for a lower order polynomial are always a subset of the those of a higher order one. Therefore, the computation of fluxes between elements of different order is carried out by using only the necessary part of the flux matrices.

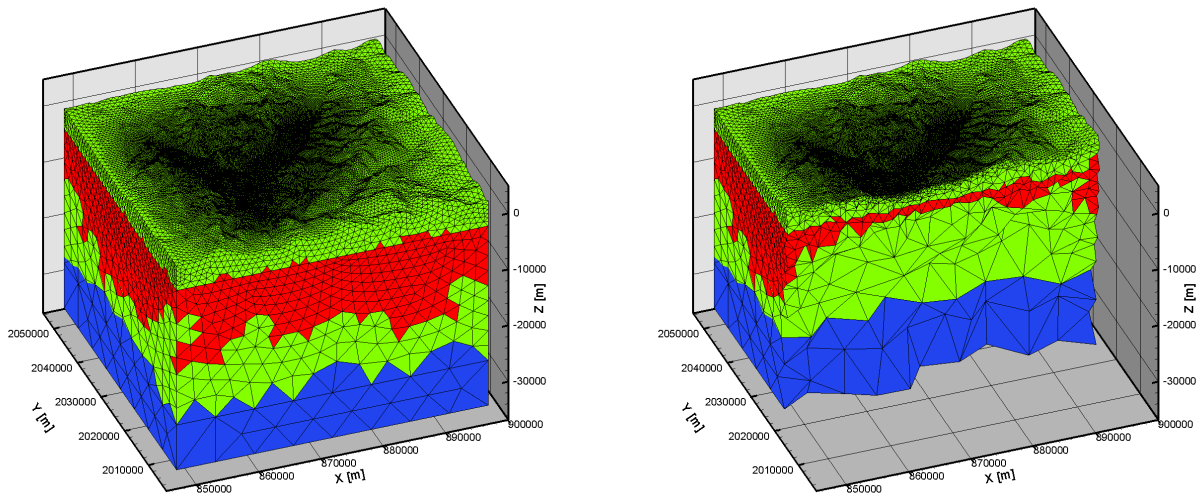


Figure 1: Tetrahedral mesh with P -adaptive elements, $P_1 = \text{blue}$, $P_2 = \text{green}$, $P_3 = \text{red}$.

Due to the direct coupling of the time and space accuracy via the ADER approach, the scheme automatically becomes adaptive in time accuracy, which often is referred to as P_t -adaptivity. In general, the distribution of the degree P is connected with the size h , i.e. the radius of the inscribed sphere, of the tetrahedral element such that the local P is determined by

$$P = P_{min} + (P_{max} - P_{min}) \left(\frac{h - h_{min}}{h_{max} - h_{min}} \right)^r, \quad P = P_{max} - (P_{max} - P_{min}) \left(\frac{h - h_{min}}{h_{max} - h_{min}} \right)^r, \quad (6)$$

where the choice of the power r determines the shape of the P -distribution. Note, that equation (6) P increases with increasing h , whereas in equation (7) P decreases with increasing h , which gives additional freedom for the distribution of P . An example of the distribution of P for the Grenoble benchmark simulation with $P_{min}=P1$ and $P_{max}=P3$ is given in Figure 1.

3.2. Local time stepping

Geometrically complex computational domains or spatial resolution requirements often lead to meshes with small or even degenerate elements. Therefore, the time step for explicit numerical schemes is restricted by the ratio of the size h of the smallest element and the corresponding maximum wave speed in this element. For global time stepping schemes all elements are updated with this extremely restrictive time step length leading to a large amount of iterations. With the ADER approach, time accurate local time stepping can be used, such that each element is updated by its own, optimal time step. An element can be updated to the next time level if its actual time level and its local time step Δt fulfill the following condition with respect to all neighboring tetrahedrons n :

$$t + \Delta t \leq \min(t_n + \Delta t_n) \quad (7)$$

Figure 2 is visualizing the evolution of four elements (I, II, III and IV) in time using the suggested local time stepping scheme. A loop cycles over all elements and checks for each element, if condition (7) is fulfilled. At the initial state all elements are at the same time level, however, element II and IV fulfill condition (7) and therefore can be updated. In the next cycle, these elements are already advanced in time (gray shaded) in cycle 1. Now elements I and IV fulfill condition (7) and can be updated to their next local time level in cycle 2. This procedure continues and it is obvious, that the small element IV has to be updated more frequently than the others. A synchronization to a common global time level is only necessary, when data output at a particular time level is required, e.g. as shown in Figure 2.

Information exchange between elements across interfaces appears when numerical fluxes are calculated. These fluxes depend on the length of the local time interval over which a flux is integrated and the corresponding element is evolved in time. Therefore, when the update criterion (7) is fulfilled for an element, the flux between the element itself and its neighbor n has to be computed over the local time interval:

$$\tau_n = [\max(t, t_n), \min(t + \Delta t, t_n + \Delta t_n)] \quad (8)$$

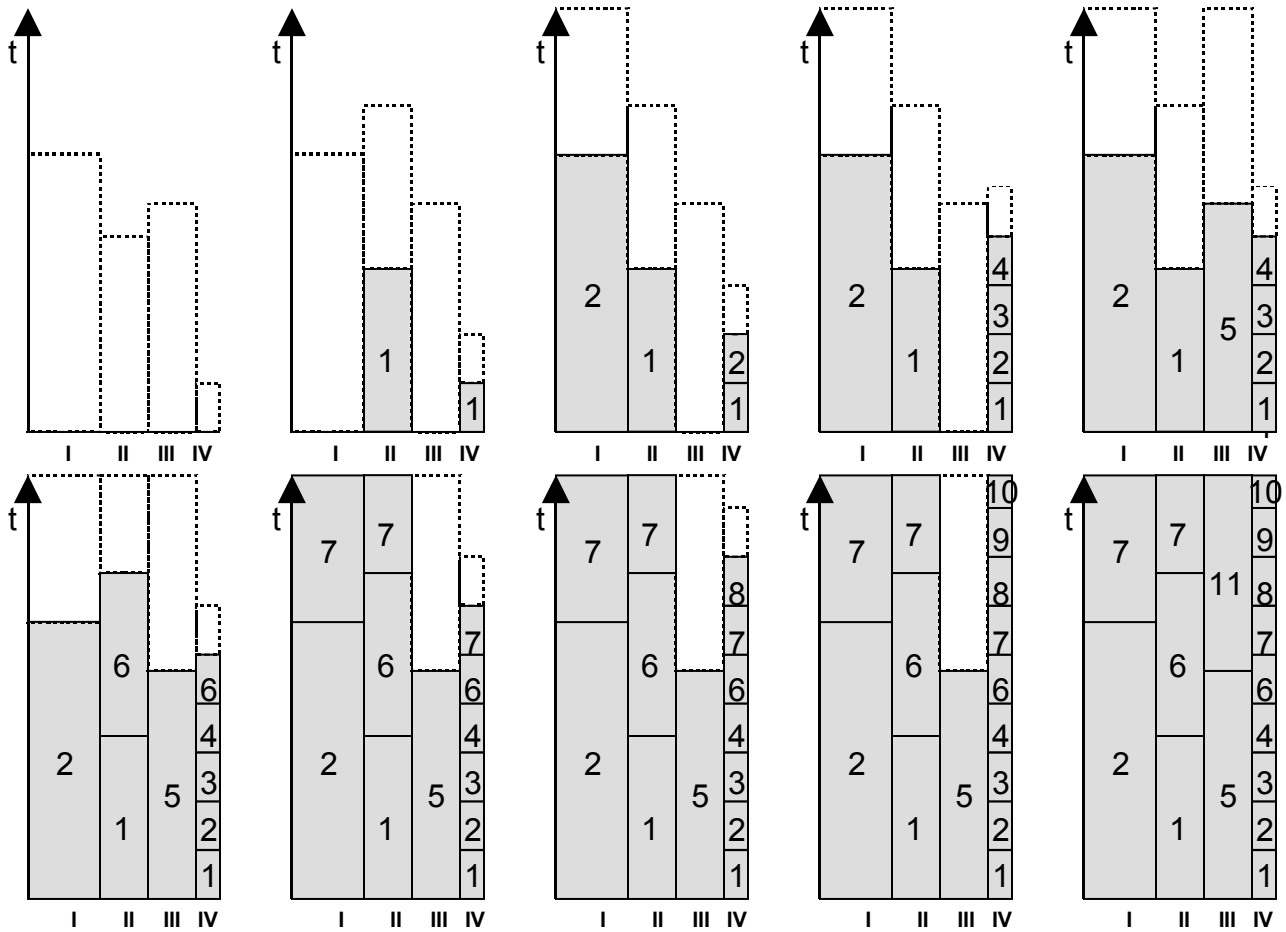


Figure 2: Visualization of the local time stepping scheme. The actual local time level t is at the top of the gray shaded area with numbers indicating the cycle, in which the update was done. Dotted lines indicate the local time step length Δt with which an element is updated.

We illustrate this on the example of the update of element III in cycle 5 (see Figure 2). The remaining part of the flux not covered by the interval in equation (8) was already computed by the neighbors during their previous local updates. These flux contributions have been accumulated and were stored into a memory variable and therefore just have to be added.

Note that e.g. element IV reaches the output time after 9 updates, which for a global time stepping scheme would require 36 updates for the four elements. With the proposed local time stepping scheme only 16 updates are necessary to reach the same output time with all elements, leading to a speedup factor of 2.25. For strongly heterogeneous local time step lengths this factor can become even more pronounced.

3.3. Mesh partitioning

For large scale applications it is essential to design a parallel code that can be run on super-computing facilities. Therefore, the load balancing is an important issue to use the available computational resources efficiently. For global time stepping schemes without P -adaptivity standard mesh partitioning as done e.g. by METIS is sufficient to get satisfying load balancing, as the unstructured tetrahedral mesh is partitioned into subdomains that contain a similar number of elements. Therefore, each processor has to carry out a similar amount of calculations. However, if P -adaptivity is applied, the partitioning is more sophisticated as one subdomain might have many elements of high order polynomials whereas another might have the same number of elements but with lower order

polynomials. Therefore, the parallel efficiency is restricted by the processor with the highest work load.

Therefore, we split the computational domain into a number of zones, that usually contain a geometrical body or a geological zone that typically is meshed individually with a particular mesh spacing and contains a dominant polynomial order. Then each of these zones is partitioned separately into subdomains of approximately equal numbers of elements, which now include both small and large tetrahedral elements with roughly the same orders of accuracy. This way, each processor receives a subdomain of each zone, which requires a similar amount of computational work. In particular, the equal distribution of tetrahedrons with different sizes is essential in combination with the local time stepping technique. Only if each processor receives subdomains with a similar amount of small and large elements, the work load is balanced. As explained in section 3.2, the large elements have to be updated less frequently than the smaller elements and therefore are computationally cheaper. We remark, that this approach increases the number of element surfaces between subdomains of different processors and therefore increases the communication required. However, communication is typically low as only the set of degrees of freedom has to be exchanged once per time step for tetrahedrons that share an interface with the boundary of a subdomain. Therefore, the improvements due to the new load balancing approach are dominant and outweigh the increase in communication.

However, we admit that the distribution of the polynomial degree P or the seismic velocity structure might influence the efficiency of the proposed partitioning technique. A profound and thorough mesh partitioning method is still a pending task as the combination of local time stepping and P -adaptivity requires a weighting strategy of the computational cost for each tetrahedral element. The automatic partitioning of unstructured meshes with such heterogeneous properties together with the constraint of keeping the subdomains as compact as possible to avoid further increase of communication is subject to future work.

In Figure 3 we show the partition of the tetrahedral mesh used for the numerical benchmark of 3-D ground motion simulation in the valley of Grenoble, where each subdomain for a processor is color-coded and consists of three parts from different geological zones.

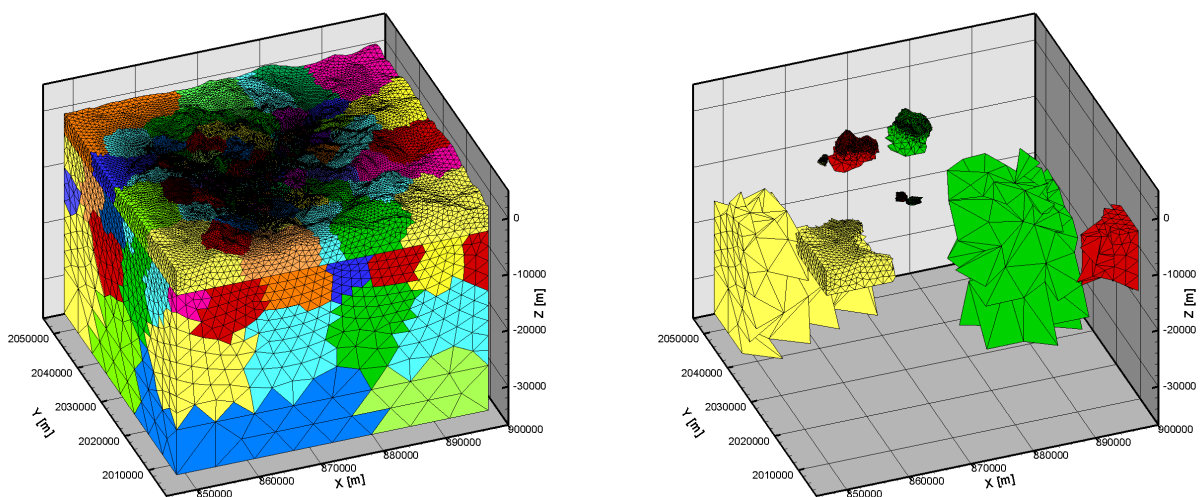


Figure 3: Partitioning of an unstructured tetrahedral mesh for 64 processors (left). Non-connected subdomains that contain a balanced number of small and large tetrahedrons from different zones (right).

4. Application Example

To confirm the performance of the proposed ADER-DG scheme and the functionality of the introduced approaches to enhance computational efficiency, we apply our new method to the strong motion case S1 as described in the benchmark of the Grenoble valley. We compute the S1 case with and without free surface topography to investigate its influence on the simulation results. The model setup is given in detail in the benchmark description and a map of the locations of the receivers and the rupture plane and the shape of the basin are shown in Figure 4.

To discretize the surface topography, we use the provided digital elevation model and resample it to a regular 500m \times 500m grid. The tetrahedral mesh discretizes the basin structure with an average tetrahedron edge length of 200m, which is gradually coarsened away from the zone of interest as illustrated in Figures 1 or 3. The rupture plane is subdivided into 15 \times 30=450 subfaults of size 300m \times 300m. The seismic attenuation properties inside the basin are approximated by viscoelastic material using three attenuation mechanisms in the frequency band from 0.1Hz to 10Hz. We decompose the model into four geometrical geological zones: (1) the basin structure, (2) the surface layer above 3km depth excluding the basin, (3) the layer between 3km and 27km depth and (4) the layer between 27km and 35km depth. The material parameters inside the basin vary as specified in the benchmark setup, whereas in the bedrock the material values vary linearly with depth.

For our simulations we distinguish the two cases of S1: FS1 denotes the *Flat* model, TS1 denotes the model with *Topography*. We use an ADER-DG scheme with *P*-adaptivity, where the following *P*-distribution is applied: zone (1) 4th order, zone (2) 4th and 5th order, zone (3) 4th and 5th order and zone (4) 3rd order. The simulation time is 30s.

First we compare the seismograms recorded at stations that are located in areas of noticeable topographic features, e.g. on mountain ridges or narrow valleys. Set (a) of receivers includes number 4, 33, 34 and 35, which are close to the rupture plane and more or less in line with its strike direction. Set (b) includes number 37, 38, 39 and 40 which are further away and more or less perpendicular to the strike. The corresponding synthetic seismograms are displayed in Figure (5), where all components v_x , v_y and v_z are unscaled within each set. For visualization, however, the amplitudes within the far receiver set (b) are scaled by a factor of 2 with respect to set (a). The comparison of the FS1 and TS1 cases in Figure (5) shows, that the incorporation of topography for TS1 generally leads to slightly larger amplitudes in the initial wave and in particular in the coda of the seismograms. Furthermore, there are phase differences as the waves in the TS1 case arrive slightly later due to the longer travel paths to higher elevations.

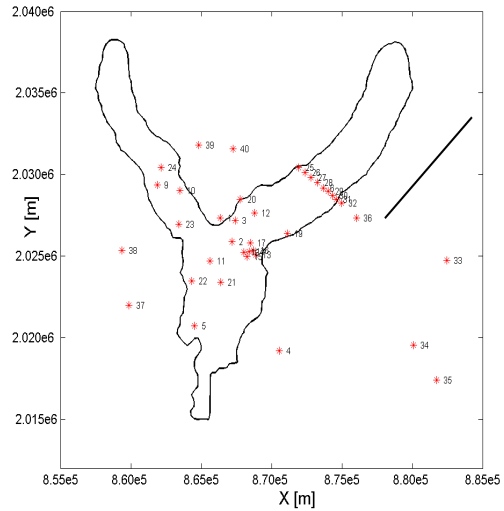


Figure 4: Receiver locations (red stars) with the location of the rupture plane (straight black line) and the shape of the basin (crooked black line).

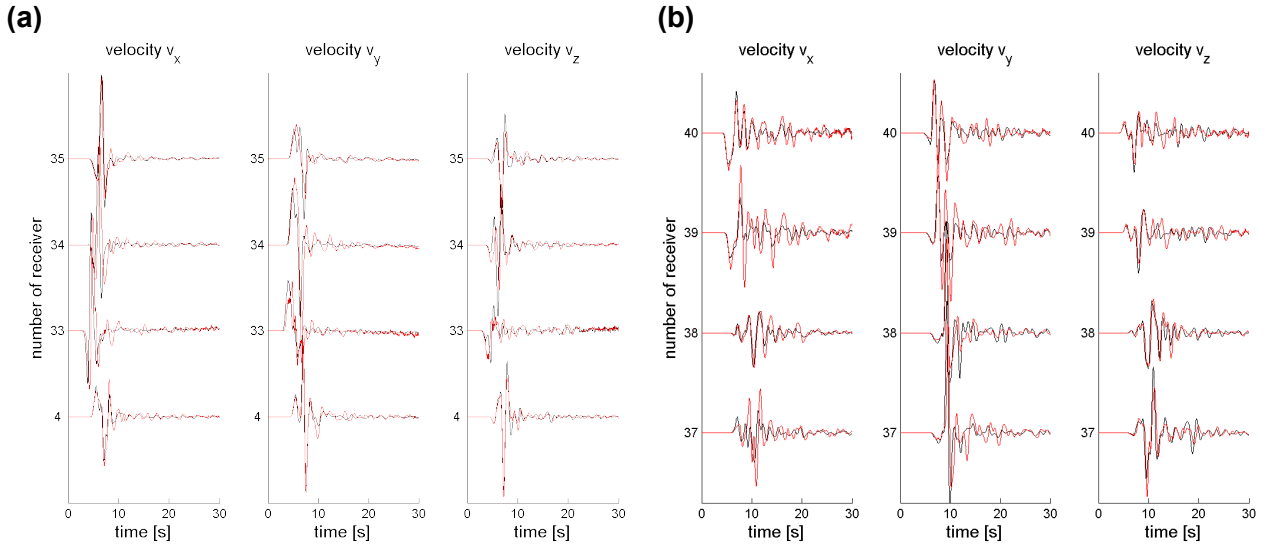


Figure 5: Comparison of seismograms of the set of near receivers (a) and far receivers (b). FS1 = black, TS1 = red.

Secondly, in Figure 6(a) and (b) we compare the seismograms along the receiver line crossing the eastern branch of the Grenoble valley together with their amplitude spectra. The differences between the FS1 and TS1 case are less pronounced, however, the spectra show slightly higher frequency contents for the TS1 case. Furthermore, receivers 32 and 36 show much smaller velocity amplitudes than the other receivers in Figure 6 as they are located on bedrock and therefore do not show the amplification effect of the sedimentary basin. We remark, that after the first wave has passed these two receivers hardly any reflection from inside the basin structure is coming back even though inside waves are scattered and reflected several times.

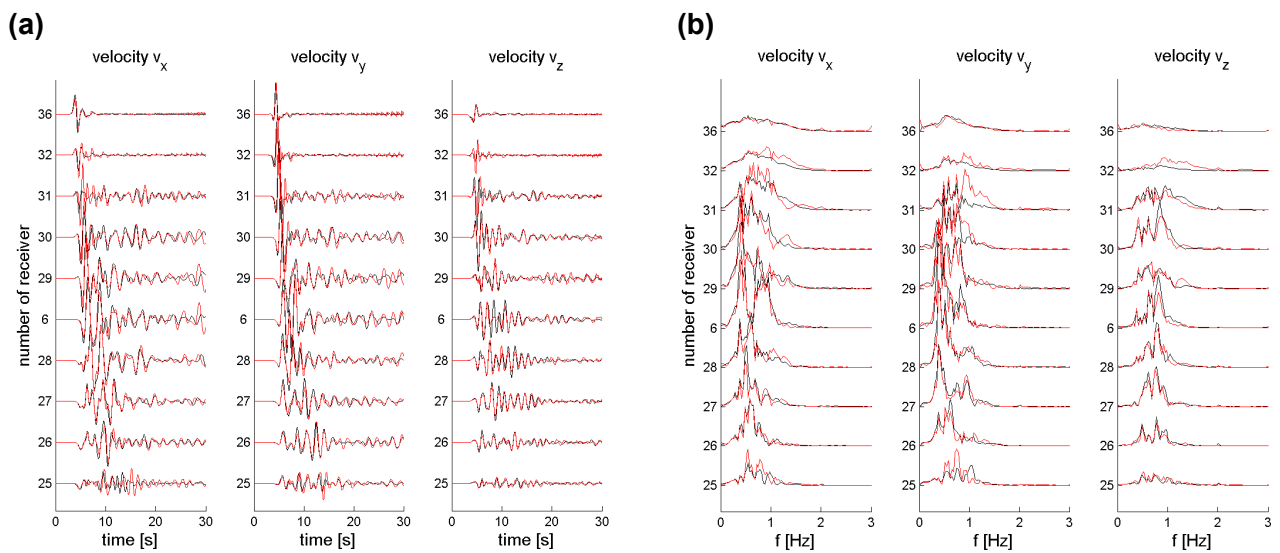


Figure 6: Velocity seismograms (a) and amplitude spectra (b) recorded on the receiver line across the valley. FS1 = black, TS1 = red.

Finally, we compare the peak ground particle motion on a regular pattern of $30 \times 30 = 900$ receivers with 1km spacing across the area of the Grenoble valley. Figure (7) shows a map of the maximum particle motion for the FS1 and TS1 case. The topography effect is mainly visible south of the rupture plane. However, in both cases the strongest ground

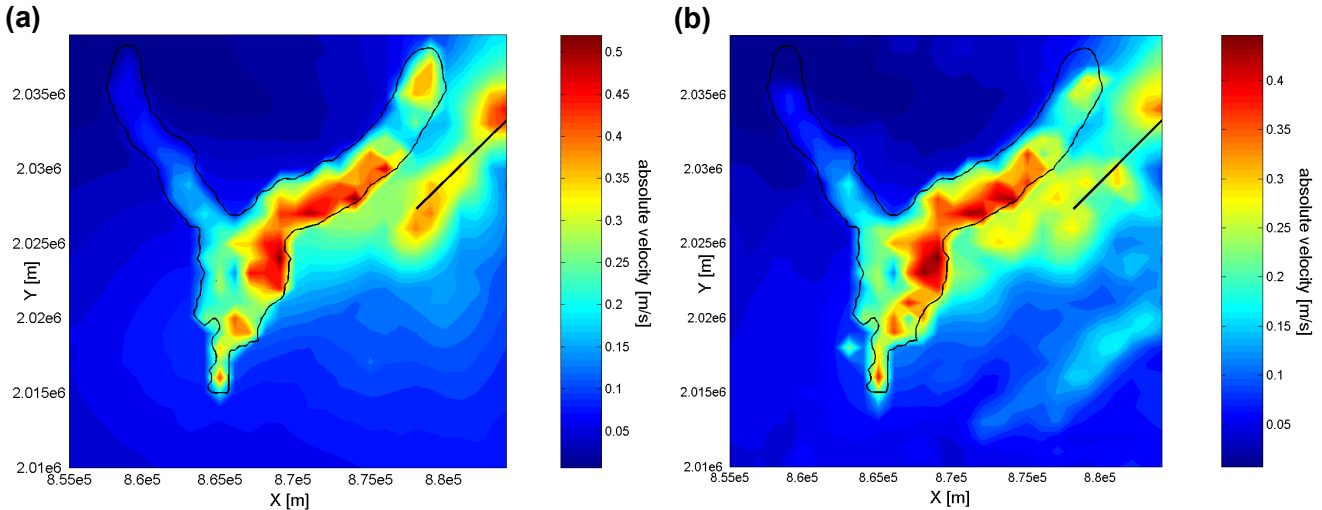


Figure 7: Map of the peak ground particle velocity for the FS1 (a) and the TS1 (b) case.

motion is predicted for the south-eastern part of the valley close to the contact of bedrock and soft sediment, which complies with observed amplification effects of sedimentary basins and the known focusing effect of along the strike direction of the rupture fault.

5. Conclusion

We presented the new ADER-Discontinuous Galerkin approach to simulate seismic wave propagation in geometrically and geologically complex media. The numerical scheme achieves high order accuracy in space and time on unstructured tetrahedral meshes and its computational efficiency is improved by applying P -adaptivity of the polynomial basis functions, local time stepping and a new mesh partitioning strategy for parallel computing. The scheme is applied to the benchmark of 3-D ground motion simulations in the valley of Grenoble and investigates the effects of topography on the simulation results. Noticeable topographic effects appear at receiver in areas of strong topography, whereas the maps of peak ground motion estimate the strongest ground motion to occur inside the basin structure at the contact of bedrock and basin sediments in strike direction of the rupture.

6. References

- Carcione, J.M., D. Kosloff and R. Kosloff (1988). Wave propagation simulation in a linear viscoelastic medium, *Geophys. J.*, 95, 597-611.
- Dumbser, M. (2005). Arbitrary High Order Schemes for the Solution of Hyperbolic Conservation Laws in Complex Domains, Shaker Verlag, Aachen.
- Dumbser, M. and M. Käser (2006). An Arbitrary High Order Discontinuous Galerkin Method for Elastic Waves on Unstructured Meshes II: The Three-Dimensional Isotropic Case, to appear in *Geoph. J. Int.*
- Emmerich, H. and M. Korn (1987). Incorporation of attenuation into time-domain computations of seismic wave fields, *Geophysics*, Vol. 52, 1252-1264.

- Käser, M., M. Dumbser (2006). An Arbitrary High Order Discontinuous Galerkin Method for Elastic Waves on Unstructured Meshes I: The Two-Dimension Isotropic Case with External Source Terms, to appear in *Geophys. J. Int.*
- Käser, M., M. Dumbser, J. de la Puente and H. Igel (2006). An Arbitrary High Order Discontinuous Galerkin Method for Elastic Waves on Unstructured Meshes III: Viscoelastic Attenuation, *submitted*
- Reed, W.H. and T.R. Hill (1973). Triangular mesh methods for the neutron transport equation, Technical Report, LA-UR-73-479, Los Alamos Scientific Laboratory.
- Toro, E.F., A.C. Millington and L.A. Nejad (2001). Towards very high order Godunov schemes, in Godunov methods; theory and applications, Kluwer Academic Plenum Publishers, Oxford, 907-940.
- Titarev, V.A. and E.F. Toro (2002). ADER: Arbitrary high order Godunov approach, *J.Sci.Comput.*, Vol. 17.609-618.